WALAILAK JOURNAL
http://wjst.wu.ac.th Health Sciences

In vitro Antioxidant Activity of Smaller Size of Coenzyme Q_{10}-Enriched Shell of Ultra-Small Nanostructured Lipid Carriers

Nuttakorn BAISAENG[1,*], Daniel PETERS[2], Michel PROST[3], Philippe DURAND[3], Rainer Helmut MÜLLER[2] and Cornelia KECK[2,4]

[1]*School of Pharmaceutical Sciences, University of Phayao, Phayao 56000, Thailand*
[2]*Institut für Pharmazie, Pharmazeutische Technologie, Biopharmazie and Kosmetik, Freie Universität Berlin, Kelchstraße 31, 12169 Berlin, Germany*
[3]*Kirial International, Laboratoire SPIRAL, Couternon, France*
[4]*Applied Pharmacy Division, University of Applied Sciences Kaiserslautern, 66953 Pirmasens, Germany*

([*]Corresponding author's e-mail: patchateeya@yahoo.com)

Received: 5 November 2015, Revised: 28 December 2015, Accepted: 16 January 2016

Abstract

CoQ_{10}-enriched shells of ultra-small nanostructured lipid carriers (usNLC), or oil with dissolved CoQ_{10} surrounding a based core of a solid lipid and oil mixture, were successfully produced using a hot high pressure homogenization technique. Then, 2 different concentrations of CoQ_{10} were loaded into usNLC, to compare the effect of particle size on antioxidant capacity. A particle size of 5.0 % CoQ_{10}-loaded usNLC (about 80 nm) was approximately 2 times larger than 0.5 % CoQ_{10}-loaded usNLC (about 50 nm), and the lightness of the yellow-colored pigment of CoQ_{10} was observable by the naked eye as regards the decrease in particle size. In addition, the spherical shape of the empty usNLC and CoQ_{10}-enriched shell of usNLC was shown by a transmission electron microscopy (TEM). Interestingly, a 10 times lower CoQ_{10} loading capacity into usNLC with a smaller size showed a higher antioxidant capacity than a higher CoQ_{10} loading and a bulk solution of CoQ_{10}, by decreasing DPPH free radical scavenging activity using the DPPH method and increasing the resistance of red blood cells to oxidative damage using a biological Kit Radicaux Libres (KRL) test. Therefore, this study suggests that the smaller particle size of CoQ_{10}-enriched shells of usNLC deserves to be developed and evaluated further *in vivo* study, in order to prove the antioxidant effects.

Keyword: CoQ_{10}-enriched shell, ultra-small nanostructured lipid carriers, antioxidant, DPPH method, KRL test

Introduction

Coenzyme Q_{10} (CoQ_{10}), which is composed of p-benzoquinone ring and polyisoprenoid side chains, belongs to the quinone group. The side chain of CoQ_{10} consists of 10 isoprene units that are responsible for the lipophilicity of the molecule, and makes the molecule of CoQ_{10} highly lipophilic [1], as shown in **Figure 1**.

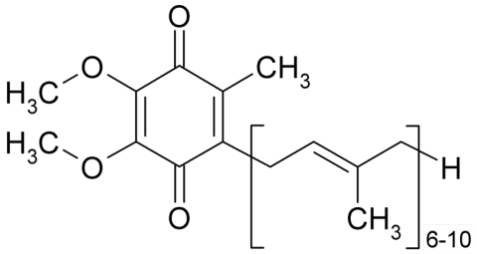

Figure 1 Chemical structure of CoQ_{10}.

Consequently, CoQ_{10} can freely penetrate into the cellular membranes, and plays an important role in electron transportation during aerobic cellular respiratory participation and adenosine triphosphate (ATP) synthesis in the mitochondria [2,3]. Furthermore, it shows a lipid antioxidant potential to protect the cells against aging induced by free radicals [4,5] and to increase the production of the basement membrane compound and the proliferation of fibroblasts as an anti-aging effect on the mitochondria cells in the skin [6]. Moreover, the dermal application of formulations containing CoQ_{10} shows a reduction in the depth of human wrinkles after a 6 month application [7]. Therefore, in recent years, CoQ_{10} is used as the main active compound for lipid antioxidant and anti-aging effects in many pharmaceutical and cosmetic products. Increasing its water solubility by a particle size reduction of CoQ_{10} may promote greater antioxidant capacity in topical drug delivery efficiency, as previous studies that reported the topical drug delivery of particle size reduction of CoQ_{10} showed higher antioxidant capacity, with deeper skin penetration than traditional CoQ_{10}-loaded emulsion [8,9].

Ultra-small nanostructured lipid carriers (usNLC) lipid-based particles with a diameter of usually less than 50 nm, were successfully developed [10] and used as a novel CoQ_{10} delivery system with a high substance solubility and stability, and with powerful skin penetration, to enhance the deeper porcine skin penetration compared to the similar particle size of nanoemulsion (NE) as the traditional lipid nanocarriers and the larger particle size of nanostructured lipid carriers (NLC) as the second generation of lipid nanocarriers at the same concentration of CoQ_{10} [11]. In addition, CoQ_{10}-loaded usNLC also exhibit a higher antiradical capacity in the biological KRL test, compared to CoQ_{10}-loaded NE and NLC [10]. In order to exclude the possibility of a different matrix effect from various lipid carriers, it is expected that solubility issues of CoQ_{10}-loaded usNLC with smaller particle size and with a 10 times lower concentration of CoQ_{10} will lead receipt of a renewed impetus of the antioxidant capacity (AOC) by using a well-known standard antioxidant measurement, i.e., the DPPH method, and a strong *in vitro* - *in vivo* correlation of antiradical analysis, i.e., the biological KRL test [12], compared to larger particle size of the same lipid matrix.

The aim of this study, therefore, was to determine the *in vitro* AOC of 0.5 % CoQ_{10}-loaded usNLC, compared to 5.0 % CoQ_{10}-loaded usNLC and a bulk solution of CoQ_{10}, by the DPPH method and the biological KRL test. In addition, the physicochemical properties, i.e., size, zeta potential, volume distribution of diameter, entrapment efficiency, drug loading capacity, morphology, and the short-term physicochemical stability of 2 different concentrations of CoQ_{10} in usNLC, were also assessed.

Materials and methods

Materials

CoQ_{10} was obtained from BIK international Handel GmbH, (Germany). Dioctyl ether (Cetiol® OE) and cetyl palmitate (Cutina® CP) were obtained from Cognis GmbH, (Germany). Caprylic/capric triacylglycerols (Miglyol® 812) was purchased from Gattefosse (Cedex, France). Polyglyceryl-3-methylglucose distearate (Tego Care® 450) was purchased from Goldschmidt (Essen, Germany). Polyoxyethylene (20) sorbitan monooleate (Tween® 80) was used as an O/W surfactant, from Uniqema

Ltd., (Belgium). W/O surfactant sorbitan monolaurate (Span® 20) was obtained from Casesar & Loretz GmbH (Hilden, Germany). For HPLC analysis, acetonitrile, acetone, and tetrahydrofuran were of HPLC grade, and were purchased from VWR Ltd., (Germany). In the case of antioxidant measurements, 2,2-Diphenyl-1-picrylhydrazyl (DPPH), the water-soluble analogue of vitamin E (Trolox®), and gallic acid were obtained from Sigma-Aldrich Co., St. Louis, (USA). The ultrapurified water was obtained from a Milli-Q Plus system, Millipore (Schwalbach, Germany). All solvents were obtained from VWR Ltd., (Germany) and used without further purification.

Methods

1. Preparation of CoQ_{10}-loaded usNLC

The compositions of 2 formulations of CoQ_{10}-loaded usNLC are presented in **Table 1**. Both formulations were produced by a hot high pressure homogenization technique, using the homogenizer LAB 40, APV Deutschland GmbH, (Germany).

Table 1 The composition of CoQ_{10}-loaded usNLC.

Composition	0.5 % CoQ_{10}-loaded usNLC (% w/w)	5.0 % CoQ_{10}-loaded usNLC (% w/w)
CoQ_{10}	0.5	5.0
Cutina® CP	1.0	1.0
Cetiol® OE	4.0	4.0
Tween® 80	2.5	2.5
Span® 20	2.5	2.5
Milli-Q water	89.5	85.0
Total	**100.0**	**100.0**

In the standard design of this machine, the homogenization operation is performed discontinuously, with a maximum batch size of 40 ml. CoQ_{10}-loaded usNLC, CoQ_{10} was dissolved into the mixture of the melted cetyl palmitate, Cetiol® OE, and Span® 20, and heated to about 50 °C. The water phase, containing Tween® 80, was heated above 5 °C of the lipid phase. To obtain the pre-emulsion, the water phase was added into the oil phase and mixed by an Ultra Turrax T25, applying 8000 rpm for 30 s. The coarse pre-emulsion was passed through the piston-gap homogenizer by applying 3 homogenization cycles at 800 bars of homogenization pressure and at 75 °C. The sample was then cooled down to an ambient temperature.

2. Particle size analysis

The particle size analysis was performed by dynamic light scattering, also known as photon correlation spectroscopy (PCS), using a Malvern Zetasizer Nano ZS (Malvern Instruments, UK) that could detect the particle size in the range of 0.6 nm to 6 μm. Prior to the measurement, all samples were diluted with distilled water in order to have a proper light scattering intensity. In 10 mm diameter disposable cells, the mean particle size was measured at an angle of 173°, and the width of the particle size distribution was performed as the polydispersity index (PI). This analysis was performed by the

Malvern software version 6.32 with general-purpose mode at 20 °C. The hydrodynamic diameter (z-average) was measured 10 times in each sample. From the particle size range of PCS analysis, the larger particles of 6 μm cannot be detected. Therefore, the low angle light scattering technique, i.e., laser diffraction, was used as an additional technique to confirm the absence of the possible large particles by using a Malvern Mastersizer 2000 that could detect the particle size in the range of 20 nm to 2 mm. The real refractive index and the imaginary index were 1.45 and 0.01, respectively. No ultrasound was applied to the samples before and during the measurement. All samples were measured 3 times, and a given size was expressed as the percentage of the volume distribution of the particles in the sample, i.e., Dv50, Dv90, Dv95, and Dv99. This means the volume distribution of the particles in the sample is equal or below 50, 90, 95, or 99, respectively.

3. Zeta potential analysis

To predict the physical stability of the samples, the electrophoretic mobility of the particles in the formulations was also determined by using a Malvern Zetasizer Nano ZS. It is directly proportional to the magnitude of the electrostatic charge on the particle, also called the zeta potential, indicating the physical stability of the colloidal systems. The zeta potential was analyzed by the laser Doppler velocimetry (LDV) and phase analysis light scattering (PALS) techniques. The medium (distilled water) for the zeta potential measurement was adjusted to get a conductivity of 50 μS/cm by using sodium chloride solution (0.9 % w/v). The pH of the medium was in the range of 5.5 - 6.0. The electric field strength (20 V/cm) was applied during the measurement. Then, the ZP was calculated with the Helmholtz-Smoluchowski equation. To obtain the precision in the measurements, all samples were measured in triplicate.

4. Transmission electron microscopy (TEM)

The morphology of the empty usNLC and CoQ_{10}-loaded usNLC was assessed by using a TEM using TECNAI G2 20 S-TWIN (FEI, USA). The samples were prepared by placing a drop of the empty usNLC and CoQ_{10}-loaded usNLC onto a 400-mesh copper grid coated with carbon film, followed by negative staining with 1.5 % phosphotungstic acid. Then, the samples were dried in air without vacuum before TEM analysis.

5. The percentage of entrapment efficiency (E.E.) and loading capacity of CoQ_{10}

The percentage of E.E. of CoQ_{10} in the usNLC was indirectly evaluated by determining the amount of CoQ_{10} in the water phase using high performance liquid chromatography (HPLC). Prior to HPLC analysis, all samples were centrifuged to separate the mixture of 2 phases by the ultracentrifugation method using the Optima^{TM} MAX-XP Ultracentrifuge, TLA-110 Optima^{TM} MAX-XP rotor from Beckman Coulter, USA. The samples were placed in the ultracentrifuge tubes. All tubes had the same weight, obtained using a digital balance. Subsequently, the samples were centrifuged at 266,000 g for 3 h at 4 °C. The amount of CoQ_{10} was then analyzed by the HPLC method, modified from Dingler (1998). The HPLC system used consisted of an auto sampler model 560, a pump system model 525, and a diode array detector model 540 (Kontron Instruments, Groß-Zimmern, Germany). This system was linked to a Kroma System 2000 v. 1.70 data acquisition and process system that also controlled the HPLC modules. 20 μl of the sample were injected onto a Betasil C8 (5 μm) 125×4 mm column with a matching pre-column (Thermo Fisher Scientific, Waltham, USA). The column was kept at room temperature during the measurement. The mobile phase consisted of acetonitrile HPLC grade (VWR, Germany) and tetrahydrofuran HPLC grade (VWR, Germany) in a ratio of 9:1 (v/v). The mobile phase was run with a flow rate of 1.5 ml/min. The UV-spectrum was recorded at a wavelength of 280 nm. The calibration curve of the bulk CoQ_{10} was obtained by the dissolved CoQ_{10} in acetone of HPLC grade. This calibration curve of the bulk CoQ_{10} in acetone served as a reference for CoQ_{10}-loaded usNLC. A linear regression was obtained by plotting the peak of the area under curve (AUC) of the bulk CoQ_{10} from HPLC versus their sequential dilution of CoQ_{10} concentration (μg/ml). The linearity of the method was confirmed over the tested concentration range (10 - 100 μg/ml). The amount of CoQ_{10} in both formulations was calculated by fitting this linear regression. Then, the amount of encapsulated CoQ_{10} in usNLC was calculated by the

difference between the total amount of CoQ_{10} in the formulation and the amount of CoQ_{10} that remained in the aqueous phase after ultracentrifugation as the indirect method, applying Eq. (1):

$$\% \text{ Entrapment efficiency (E.E.)} = (A - B)/A \times 100 \quad (1)$$

where A is the total amount of CoQ_{10} in the formulation and B is the free amount of CoQ_{10} in the aqueous phase. In addition, the percentage of drug loading capacity (% D.L.) was calculated according to the Eq. (2) as drug entrapped in lipid nanocarriers (A – B) versus the total amount of the lipid used in the formulation (C):

$$\% \text{ Drug loading capacity (D.L.)} = (A - B)/C \times 100 \quad (2)$$

***In vitro* antioxidant capacity measurements**

1. DPPH method

DPPH is a simple method for measuring the radical scavenging activity of antioxidants against free radicals like the 2,2-diphenyl-1-picrylhydrazyl radical ($DPPH^{\bullet}$). This analytical method has been developed to determine the antioxidant activity of many compounds in pharmaceutical products and foods utilizing the stable radical of DPPH ($DPPH^{\bullet}$). The $DPPH^{\bullet}$ solution is purple in color, and the odd electron in the $DPPH^{\bullet}$ gives a strong absorption maximum at 517 nm. When the odd electron of $DPPH^{\bullet}$ becomes paired with a hydrogen from a free radical scavenging antioxidant to form the reduced DPPH-H, the decolorization of $DPPH^{\bullet}$ solution is obtained. These solution mixtures were kept in the dark for 30 min and the absorbance of $DPPH^{\bullet}$ solution was measured at 517 nm using a Shimadzu UV-1700 PharmaSpec spectrometer (Shimadzu Europe GmbH, Germany). DPPH solution (0.1 mg/ml, 2 ml) was used as a blank. An easy way to present the antioxidant activity of active compounds would be to compare it with a common reference standard. One common reference standard (2R)-2,5,7,8-Tetramethyl-2-[(4R,8R)-(4,8,12-trimethyltridecyl)]-6-chromanol, also known as α-Tocopherol, serves this purpose. To compare antioxidant capacity between the samples and a reference standard, a suitable series of 5 dilutions of each sample (0.6 - 3.9 mmol/l) and a reference standard (5.8 - 230 µmol/l) was prepared. The procedure for measurements was the following; the different concentrations of the samples and the reference standard were added into disposable cuvettes of $DPPH^{\bullet}$ solution (2 ml) for 60 min at ambient temperature, and the changes of absorbance were recorded at 1, 3, 5, 10, 15, and 60 min. Then, the antioxidant capacity was obtained through a linear regression of data corresponding to 5 different concentrations of the samples, and was expressed in the effective concentration to reduce 50 % of the initial absorbance of $DPPH^{\bullet}$ (EC_{50} value) compared to the reference standard.

2. The biological KRL test

The antiradical capacity of CoQ_{10}-loaded usNLC was assessed by the KRL biological test. The KRL test [13] allows the dynamic evaluation of the resistance of red blood cells against the free radicals induced by 2 2'-azobis (2-amidinopropane) hydrochloride (AAPH). According to French patent no. 2,642,526, blood samples were obtained from a healthy pig in Laboratoires Spiral, France, with a half-hemolysis time near to the median reference value (±3 %) that was found in the piglets [14]. The blood solutions were diluted 1:50 in phosphate buffer in isotonic conditions at pH 7.4 and incubated at 37 °C with the different range of concentrations of CoQ_{10}-loaded usNLC (from 0 to 1 ml by liter of a reaction medium) compared to the bulk CoQ_{10}. The hemolysis was recorded by optical density decay using the KRL reader. The resistance of whole red blood cells to free radical attack was expressed by the time that was required to reach 50 % of the maximal hemolysis ($HT_{1/2}$). It was then standardized in Trolox® equivalents (a range from 0 to 1000 µmole/l of Trolox®, MW 250.29 g/mole) and in gallic acid equivalents (a range from 0 to 500 µmole/l of gallic aid, MW 170.12 g/mole). The student t-test was used to analyze the differences of antiradical capacity between 0.5 % and 5.0 % CoQ_{10}-loaded usNLC.

3. Short-term physicochemical stability of CoQ_{10}-loaded usNLC

To evaluate the physicochemical stability of CoQ_{10}-loaded usNLC, the samples were stored at 4, 20, and 40 °C for 3 months. The hydrodynamic particle size, zeta potential, and the amount of CoQ_{10} in the formulations were analyzed at day 1, 15, 30, and 90. The main reason to measure the hydrodynamic particle size was to assess the phase separation of samples due to coalescence of the lipid nanoparticles. In addition, the ZP could be used for predicting the physical stability of the usNLC during the study period and in long-term storage time. The particle size analysis and ZP measurement have been described in detail above. Otherwise, the different volumes of CoQ_{10}-loaded usNLC were sampled and adjusted to obtain the same final concentration of the active compound. Then, the remaining amount of CoQ_{10} in the formulations was directly analyzed during the period of study by HPLC.

Statistical analysis

All results are presented as the mean ± standard deviation of 3 or more experiments. The statistical analysis was performed by using the independent t-test for 2 samples comparison and one-way ANOVA for 3 samples comparison at a significance level of 0.05.

Results and discussion

Particle size analysis

Two different concentrations of CoQ_{10}-loaded usNLC were successfully produced from the mixture of freely compatible solid lipid, i.e., cetyl palmitate, in liquid lipid, i.e., dioctyl ether, and the mixture of Tween® 80 and Span® 20, by a hot high pressure homogenization technique. Of special interest is the macroscopic appearance of 0.5 % CoQ_{10}-loaded usNLC transparent, compared to 5.0 % CoQ_{10}-loaded usNLC. This can be explained by a previous study; transparency can be obtained if a droplet size of the preparation of less than 60 nm can be achieved [15], and this small droplet size of CoQ_{10}-loaded usNLC will no longer scatter the light. Somehow, CoQ_{10} still absorbs light and, therefore, these preparations look orange, as shown in **Figure 2**, and the lightness of the colored pigments of CoQ_{10} was increased when the concentration of CoQ_{10} was decreased.

Figure 2 Macroscopic appearance of 0.5 % CoQ_{10}-loaded usNLC (left) and 5.0 % CoQ_{10}-loaded usNLC (right).

This result related to the PCS analysis, where the particle size of the usNLC with a 10 times lower concentration of CoQ_{10} was approximately 50 nm, that is, below 60 nm, resulting in a translucent apperance, whereas the usNLC containing 5 % CoQ_{10} appeared opaque, as the particle size of dispersions were around 80 nm on the day of production (Day 0) as shown in **Table 2**.

Table 2 The particle size and zeta potential of 0.5 % and 5.0 % CoQ_{10}-loaded usNLC by PCS and LD analysis at 20 ± 2 °C for 90 days (PI is a size distribution, and Dv is a volume distribution of diameter).

Samples	PCS analysis		LD analysis				Zeta potential (mV)
	Size (nm)	PI	Dv10 (nm)	Dv50 (nm)	Dv90 (nm)	Span value	
0.5 % CoQ_{10}-loaded usNLC							
- Day 0	47	0.157	81	121	181	0.826	−20
- Day 90	46	0.145	85	127	184	0.779	−20
5 %CoQ10-loaded usNLC							
- Day 0	81	0.132	84	127	187	0.811	−35
- Day 90	80	0.134	84	128	189	0.820	−34

In addition, both formulations exhibited values of the PI below 0.2, indicating a narrow size distribution. However, PCS measurement could detect the particles in the limit range of 20 nm to 2 μm. LD was an additional technique for proving the disappearance of the possibility of large particles for 90 days at room temperature. The given particle size is expressed in the volume distribution, such as Dv50, Dv90, Dv95, and Dv99. The larger particles of 5 % CoQ_{10}-loaded NLC were shown in Dv50, Dv90, Dv95, and Dv99, compared to a 10 times lower concentration of CoQ_{10} in usNLC. In addition, the span value was a statistical parameter, useful for characterizing the particle size distribution, and was calculated by using the reference equation:

$$\text{Span} = (\text{Dv90} - \text{Dv10})/\text{Dv50} \quad (4)$$

A span value of less than 2 indicates a narrow size distribution and polydispersity. From the LD results, it proved that there was a narrow size distribution (span < 2) and no particles larger than 1 μm in both formulations of CoQ_{10}-loaded usNLC during the study period, as shown in **Table 2**.

Zeta potential analysis

The zeta potential can be used to predict the physical stability of the colloidal dispersion systems. Nanodispersions with zeta potential values either more positive than +30 mV or more negative than -30 mV are expected to possess good physical stability. This is a useful strategy for increasing the physical stability of nanodispersions stabilized by electrostatic stabilization from ionic-emulsifying agents. On the other hand, in the case of nonionic stabilizers, a steric stabilization effect obviously influences the physical stability of the colloidal dispersion systems. In most cases, both mechanisms complement each other and, therefore, in the case of nonionic stabilizers, use of zeta potential values either more positive than +20 mV or more negative than −20 mV are sufficient to stabilize the colloidal nanodispersion systems [16]. In this study, Tween® 80 and Span® 20 were used as nonionic stabilizers. Thus, zeta potentials of approximately −20 mV for 0.5 % CoQ_{10}-loaded usNLC and −35 mV for 5.0 % CoQ_{10}-loaded usNLC should have efficiently stabilized the nanodispersions by the steric and electrostatic effects.

According to the PCS and zeta potential results, increasing the amount of CoQ_{10} in the particles led to an increase in the mean particle size and the absolute value of zeta potential, as shown in **Table 2**. The increase either in particle size or the absolute value of zeta potential was associated with the frontier of the matrix saturation with the accumulation of the drug at the particle surface. This also impacted on the zeta potential, which became more negative, indicating good physical stability during the study period of time.

TEM

Understanding a clear picture of the particle structure would involve specifying the particle surfaces or the particle interfaces in the sample. Typically, the microscopic image provides a tremendous amount of information, and a simplification technique is needed to identify the structure of the very small molecule. A standard light microscope cannot be used to view the structure of the particle size of CoQ_{10}-loaded usNLC, since the particles are actually smaller than the shortest wavelength of visible light. Consequently, there are other types of microscopes, such as electron microscopes, that can provide the much greater magnifications needed in order to see the small objects as nanoscale. TEM is an interesting advancement in electron microscopes, used for determination of the area of the real-space of nanoparticle structures [17] and the surface characterization of liquid samples [18]. Therefore, the assessment of the morphology and the surface structure of CoQ_{10}-loaded usNLC were compared to the empty usNLC by TEM. **Figure 3** depicts the morphology and surface structural details of particulate objects of the empty usNLC (left) and CoQ_{10}-loaded usNLC (right). Concerning the negative staining process, the phosphotungstic acid surrounds the particles with electron-dense deposits and reveals the surface by the contrast between the stain (dark) and the objects (light). Therefore, the morphology of the empty usNLC and CoQ_{10}-loaded usNLC are shown as the light color.

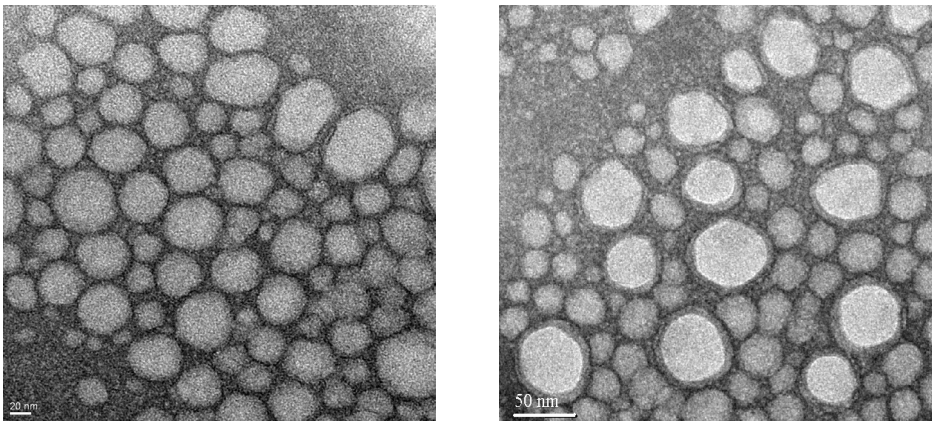

Figure 3 Morphology of the empty usNLC (left) and CoQ_{10}-loaded usNLC (right) under TEM analysis.

From the TEM image, almost spherical particles in the empty usNLC and CoQ_{10}-loaded usNLC are observed. This is in agreement with a previous study that also discovered the spherical shape of lipid nanoparticles by using an electron microscope, i.e., cryo-field emission SEM (cryo-FESEM) [19]. Concerning the TEM results, it was interestingly that CoQ_{10}-loaded usNLC has a dark ring around the outer shell of the particles on the TEM image, whereas it is not found in the case of the empty usNLC. This might be explained by the differing solubility of CoQ_{10} in oil and solid lipid. Many drugs show a higher solubility in oils than in solid lipids. Thus, CoQ_{10} can be dissolved in oil, and the amount of dioctyl ether exceeds the amount of cetyl palmitate, more than in solid lipid. Although a homogeneous system of a free solubility of solid lipid in the oil molecules occurred in the emulsification process during their production, the solid lipid had a high melting point, which could have resulted in solidification in room temperature, and therefore in phase separation. It forms the new type of nanolipid carriers impressed as drug-enriched shell. These “core-shell nanoparticles” can be considered as analogous to O/W emulsion, as they have solid-in-oil-in-water dispersion. This is very valuable information for distinguishing the morphology and the surface structure of CoQ_{10}-loaded usNLC from the empty usNLC, and it provides a necessary intellectual data and a key structural concept that will enable an increase in basic knowledge for the scientific forecast of perspectives and the potential for novel structures for lipid-based nanocarriers.

E.E. and loading capacity of CoQ_{10}

In order to assess the E.E. of CoQ_{10} in the usNLC, CoQ_{10} was encapsulated as a model drug, and the separation of the lipid phase from the aqueous phase was required for all samples. This was performed by ultracentrifugation, and an example of CoQ_{10}-loaded usNLC after ultracentrifugation is shown in **Figure 4**.

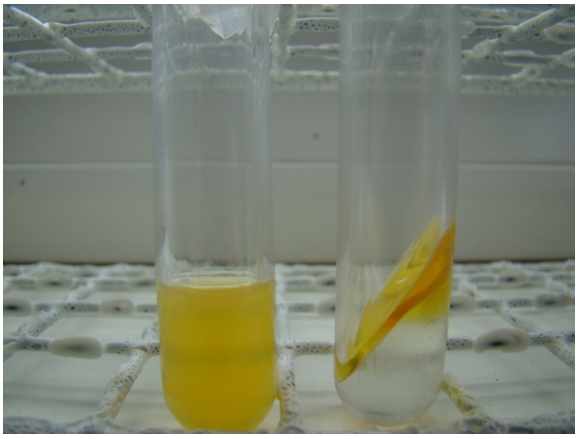

Figure 4 CoQ_{10}-loaded usNLC after ultracentrifugation.

As an indirect method for ascertaining entrapment efficiency, the remaining amount of CoQ_{10} in the aqueous part (the bottom clear part in the test tube, as shown in **Figure 4**) of both formulations was then analyzed by HPLC. According to the HPLC results, the entrapment efficiency of both formulations of CoQ_{10} in the usNLC was assumed to be approximately 100 % by the calculation of Eq. (1), since no peak of CoQ_{10} was detected in the aqueous phase by HPLC. This result was in agreement with previous studies, where the entrapment efficiency of CoQ_{10} into NLC and NE was approximately 100 % [20,21]. In addition, a previous study reported that CoQ_{10} could not be detected in the aqueous phase, because its solubility was less than 4 ng/ml [22]. Otherwise, it might be due to the limit of detection (LOD) of HPLC, which was found to be 0.33 µg/ml. On the other hand, the percentage of CoQ_{10} loading capacity was calculated by Eq. (2). It was found that 5 % CoQ_{10}-loaded usNLC exhibited approximately a 10 times higher loading capacity of CoQ_{10} than another formulation with the same type of lipid matrix used, as shown in **Table 3**.

Table 3 The percentage of entrapment efficiency (E.E.) and loading capacity (D.L.) of CoQ_{10} in usNLC (n = 3).

Formulation	Composition						
	CoQ_{10} (% w/w)	**Lipid** (% w/w)	**Surfactant** (% w/w)	**Water q.s.** (% w/w)	**E.E.** (%)	**D.L.** (%)	**AUC***
0.5 % CoQ_{10}-loaded usNLC	0.5	5.0	5.0	100.0	100.0	10.0	16.6 ± 0.1
5.0 % CoQ_{10}-loaded usNLC	5.0	5.0	5.0	100.0	100.0	100.0	15.9 ± 0.2

AUC*- Area under the curve of CoQ_{10} in both formulations at the same concentration by HPLC analysis

Although 5 % CoQ_{10}-loaded usNLC had a higher loading capacity, the AUC, that is, the mathematically integrated area under the concentration-time curve which is represented in the amount of the drug, was slightly less than 0.5 % CoQ_{10}-loaded usNLC at the same concentration of the active compound. This meant the smaller particles usually yielded a higher drug concentration compared to the larger ones, due to an increase in the solubility of the drug with a higher number of CoQ_{10} nanoparticles.

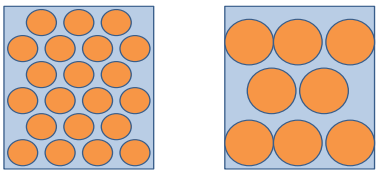

Figure 5 The model of the different number of particles between 0.5 % CoQ_{10}-loaded usNLC (left) and 5 % CoQ_{10}-loaded usNLC (right) in the same volume fraction.

To be clear on this point, **Figure 5** shows the model of the different number of particles with CoQ_{10} between the smaller particles (left) and the larger particle (right) in the same volume fraction. This implied that the smaller particles of 0.5 % CoQ_{10}-loaded usNLC should have had a higher number of nanoparticles than 5 % CoQ_{10}-loaded usNLC at the same concentration. In agreement with this result, a previous study also reported that a sharp decrease in particle size resulted in a higher drug concentration [23].

Antioxidant capacity

1. DPPH method

The CoQ_{10} which was used in this study, bright orange in color, was ubidecarenone, or ubiquinone. This is an oxidized form of CoQ_{10} and acts as the lipid soluble endogenous antioxidant in most eukaryotic cells. Nevertheless, endogenous CoQ_{10} *in vitro* can be presented in aqueous, hydrophobic, or intermediate environments as pro-oxidative molecules. To assess the reactivity of CoQ_{10} in the usNLC with $DPPH^{\bullet}$, the antioxidant capacity of CoQ_{10}-loadd usNLC was measured by a decrease in the absorbance of $DPPH^{\bullet}$, and expressed in the percent inhibition of DPPH. Thus, the samples that could lower the initial absorbance of $DPPH^{\bullet}$ solution by 50 % (EC_{50}) were chosen as the endpoint for measuring the antioxidant activity. This change was compared to the change induced by the reference standard (α-Tocopherol), and the antioxidant capacity of the sample was expressed in micromoles of α-Tocopherol equivalents per 100 gm of sample or α-Tocopherol units per 100 gm. According to the results, 0.5 % CoQ_{10}-loaded usNLC had an EC_{50} of 2.12×10^{-3} mole/l, and 5 % CoQ_{10}-loaded usNLC had an EC_{50} of 2.42×10^{-3} mole/l, as shown in **Figure 6**, and both formulations had a 2 times higher EC_{50} than the bulk solution.

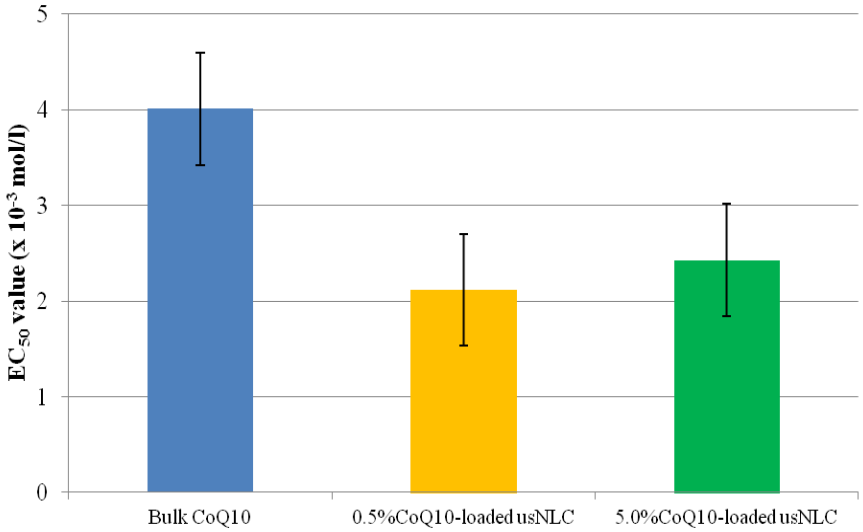

Figure 6 Comparison of the EC_{50} of 0.5 % CoQ_{10}-loaded usNLC, 5 % CoQ_{10}-loaded usNLC and the bulk solution by DPPH method (n = 3).

This means 0.5 % CoQ_{10}-loaded usNLC had a higher antioxidant capacity than 5 % CoQ_{10}-loaded usNLC that contained a higher concentration and drug loading capacity in the formulation and the bulk CoQ_{10}, respectively. These results might have been caused by the different solubility of CoQ_{10} in the formulation, so that the smaller particles exhibited a higher AUC leading, to a higher antioxidant capacity. This could be confirmed by the HPLC results, where 0.5 % CoQ_{10}-loaded usNLC showed a higher AUC than another. However, both formulations had a higher value of EC_{50} than α-Tocopherol (EC_{50} = 0.34×10^{-3} mmol/l). This means both formulations had a lower antioxidant capacity than the reference standard. It could be associated with the lipophilic/hydrophilic characteristics of the compounds, and could also be associated with the matrix of the active ingredients. However, this fact does not mean that CoQ_{10}-loaded usNLC had insufficiently reactive properties. In agreement with these results, the radical protecting activity of CoQ_{10} was found to be significantly lower as compared to vitamin E when these antioxidants operated in peroxidizing lipid membranes [24]. This is contrary to a previous study, where ubiquinone and vitamin E were equally effective in scavenging lipid radicals [24]. This discrepancy revealed that the antioxidant capacity of CoQ_{10} might have been compulsorily linked to the formation of split products counteracting the DPPH free radical effect, while the reference standard directly reacted with the DPPH free radical.

2. The biological KRL test

In addition to the *in vitro* DPPH radical scavenging method, the *in vitro* antioxidant potential of CoQ_{10}-loaded usNLC was also assessed, comparing to the bulk solution by using the KRL biological test. The antiradical efficiency of the samples was expressed in the half-hemolysis time ($HT_{1/2}$) of the control blood compared to the bulk solution of CoQ_{10}, as shown in **Figure 7**.

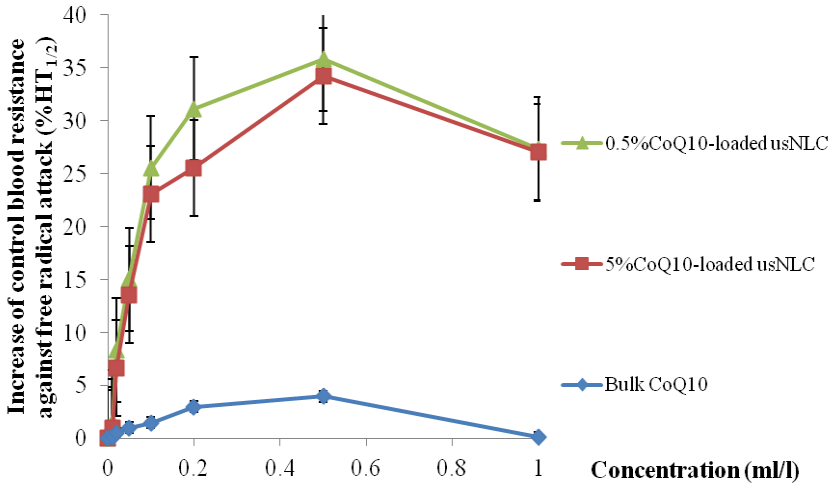

Figure 7 Comparative antiradical capacity of 0.5 % CoQ_{10}-loaded usNLC, 5 % CoQ_{10}-loaded and the bulk solution by the biological KRL test (n = 3).

It was found that the antiradical capacity was highly dependent on the concentration of CoQ_{10}. The increase in the $HT_{1/2}$ of control blood against the free radicals of both formulations of CoQ_{10}-loaded usNLC was significantly different from the bulk solution ($p < 0.05$), whereas no significant difference of the $HT_{1/2}$ of the control blood was found in 5 % CoQ_{10}-loaded usNLC and 0.5 % CoQ_{10}-loaded usNLC ($p > 0.05$). Nevertheless, the trend of the $HT_{1/2}$ of control blood against the free radicals of 0.5 % CoQ_{10}-loaded usNLC was slightly higher than 5 % CoQ_{10}-loaded usNLC. This result related to the above result of the AUC of CoQ_{10} under HPLC analysis and the *in vitro* antioxidant capacity of DPPH measurement. These results agree with a previous study, where a maximum of the antiradical capacity was reached when a concentration of CoQ_{10} in both formulations and the bulk CoQ_{10} was 0.5 ml/l [10], and in which both formulations of CoQ_{10}-loaded usNLC possessed a 9-fold higher antiradical capacity compared to the bulk solution. This result indicated that a possibility of a pro-oxidative effect of CoQ_{10} was achieved with a decrease in particle size, possessing a larger surface aea and a higher reaction rate, leading to an increase in the solubility of the active compound, consequently achieving a higher antiradical capacity. In addition, 0.5 % CoQ_{10}-loaded usNLC showed the highest antiradical capacity, compared to 5 % CoQ_{10}-loaded usNLC and the bulk solution. The results were expressed in terms of Trolox® equivalent and gallic acid equivalent antioxidant capacity, as shown in **Figure 8**.

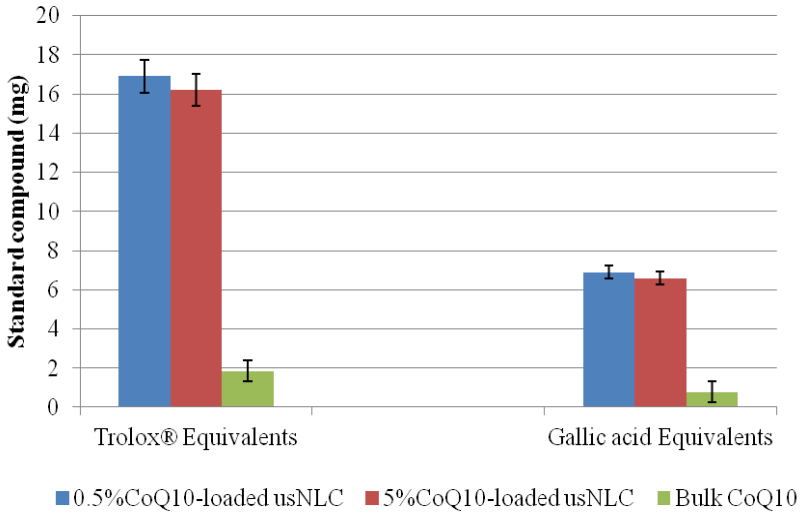

Figure 8 Trolox® and Gallic acid equivalent antioxidant capacity of 0.5 % CoQ_{10}-loaded usNLC and 5 % CoQ_{10}-loaded usNLC (n = 3).

The antioxidant capacity of 0.5 % CoQ_{10}-loaded usNLC (about 16.9 mg of Trolox® equivalent value and 6.9 of gallic acid equivalent value) was very slightly significantly different from 5 % CoQ_{10}-loaded usNLC (approximately 16.2 mg of Trolox® equivalent value and around 6.6 of gallic acid equivalent value). Both formulations exhibited a 9-fold superiority in Trolox® equivalent and an 8-fold superiority in gallic acid equivalent compared to the bulk CoQ_{10} solution, which showed 1.8 mg of Trolox® equivalent value and 0.8 of gallic acid equivalent value. Consequently, both formulations of CoQ_{10}-loaded usNLC possessed a good antioxidant capacity in the standard DPPH method and the biological KRL test.

In fact, the primary function of ubiquinol ($CoQ_{10}H_2$) as an exogenous antioxidant is to donate hydrogen atoms to a radical species and, thus, remove the radical from any initiation reactions. $CoQ_{10}H_2$ becomes semiubiquinone ($CoQ_{10}H$) or ubiquinone (CoQ_{10}) after donating both hydrogen atoms [25]. CoQ_{10} could possibly function as a free radical scavenger, although it is not as efficient an antioxidant as a hydrogen donor which reacts with free radicals and lowers their activation energy; the reactivity of free radicals is then reduced. In addition, the nonconjugated arrangement of the double bonds in the CoQ_{10} tail would suggest that it would be a relatively poor free radical scavenger. For that reason, there was a question of the ability of CoQ_{10} to act as the pro-oxidative or exogenous antioxidant in this study. The antioxidant behavior of CoQ_{10} could be due to its ability to scavenge DPPH and AAPH free radicals by a hydrogen donor. It could be described by the influence of a decrease in the particle size of CoQ_{10} in nanolipid carriers leading to the change of the CoQ_{10} structure, since CoQ_{10} possesses a flexible side chain that may facilitate a reversible reduction of quinone groups and conversion to chromenol via cyclization with an isoprene unit [26]. This is in agreement with a previous study which reported that a stronger antioxidant capacity of the biological substance was obtained when decreasing the particle size [27,28]. The possibility that it can function this way in pharmaceutical or cosmetic products should be explored, since the oxidized form of CoQ_{10} predominates as the lipid soluble endogenous antioxidant in most eukaryotic cells.

The data of the standard DPPH method and the biological KRL test proved that CoQ_{10} can behave as a pro-oxidative or exogenous antioxidant. The presence of the smaller sized particles with a higher concentration of CoQ_{10}-loaded usNLC is critical to an improved antioxidant capacity of CoQ_{10} in nanolipid carriers. However, further *in vivo* studies should be probed to confirm the *in vitro* results and to carry out the specific mechanism underlying antioxidant effects of CoQ_{10}-loaded usNLC.

3. Short-term physicochemical stability of CoQ_{10}-loaded usNLC

CoQ_{10}-loaded usNLC were stored in the dark at 3 different temperatures (4 ± 2, 20 ± 2, and 40 ± 2 °C), according to a previous study which reported that the degradation of CoQ_{10} was remarkable by accelerated light exposure [29]. The samples were stored at 3 different temperature conditions over a period of 3 months. For the physical stability, the measurement of the mean hydrodynamic particle size and the surface charge of CoQ_{10}-loaded usNLC were evaluated by using a Zetasizer Nano ZS. During the storage time period, the mean hydrodynamic particle size of both formulations of CoQ_{10}-loaded usNLC was stable at 4 ± 2, 20 ± 2 °C, whereas an increase in the particle size was found at an elevated temperature, as shown in **Tables 4** and **5**. It could be stated that the high-temperature storage of samples induced the growth of the particles, due to a simulation of the Brownian motion movement of the particles, which had a higher kinetic energy at an elevated temperature. These results related to the macroscopic appearance of both formulations, meaning that they had good stability at 4 ± 2 and 20 ± 2 °C, whereas phase separation and physical color change were found in 0.5 % CoQ_{10}-loaded usNLC and in 5 % CoQ_{10}-loaded usNLC at 40 ± 2 °C, as shown in **Figure 9**.

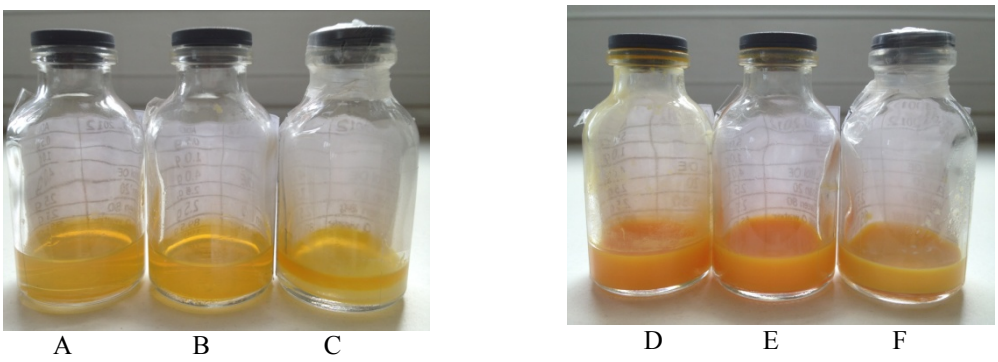

Figure 9 Macroscopic appearance of 0.5 % CoQ_{10}-loaded usNLC and 5 % CoQ_{10}-loaded usNLC at different temperatures for 90 days (A: 0.5 % CoQ_{10}-loaded usNLC at 4 ± 2 °C, B: 0.5 % CoQ_{10}-loaded usNLC at 20 ± 2 °C, C: 0.5 % CoQ_{10}-loaded usNLC at 40 ± 2 °C, D: 5 % CoQ_{10}-loaded usNLC at 4 ± 2 °C, E: 5 % CoQ_{10}-loaded usNLC at 20 ± 2 °C, and F: 5 % CoQ_{10}-loaded usNLC at 40 ± 2 °C).

In contrast, the zeta potentials more positive than +30 mV or more negative than −30 mV are normally considered as showing good physical stability for pharmaceutical or cosmetic products. As per the results, the zeta potential of 0.5 % CoQ_{10}-loaded usNLC was in the range of approximately −19 to −24 mV, and 5 % CoQ_{10}-loaded usNLC was in the range of approximately −29 to −34 mV, in the different temperature storage conditions for 3 months. It could be stated that 5 % CoQ_{10}-loaded usNLC might be more stable than 0.5 % CoQ_{10}-loaded usNLC. Nevertheless, both formulations contain nonionic stabilizers that can stabilize the nanolipid system by steric stabilization and electrostatic synergy. Consequently, in this case, the zeta potential values of either more positive than +20 mV or more negative than −20 mV were sufficient to stabilize the nanodispersion systems [16].

Table 4 Particle size and zeta potential of 0.5 % CoQ10-loaded usNLC by PCS analysis at 3 different storage conditions for 3 months (z-average is a mean diameter and PI is a size distribution).

Storage conditions	Parameter	Day 1	Day 15	Day 30	Day 90
4 ± 2 °C	**z-average (nm)**	47 ± 1	48 ± 1	48 ± 0	47 ± 1
	PI	0.19 ± 0.02	0.17 ± 0.03	0.17 ± 0.03	0.16 ± 0.03
	zeta potential (mV)	–21 ± 2	–23 ± 4	–23 ± 1	–23 ± 2
20 ± 2 °C	**z-average (nm)**	48 ± 1	48 ± 1	48 ± 1	46 ± 1
	PI	0.16 ± 0.02	0.17 ± 0.02	0.16 ± 0.02	0.16 ± 0.03
	zeta potential (mV)	–20 ± 2	–24 ± 2	–22 ± 2	–20 ± 2
40 ± 2 °C	**z-average (nm)**	54 ± 1	61 ± 1	64 ± 1	102 ± 59
	PI	0.12 ± 0.01	0.12 ± 0.02	0.18 ± 0.03	0.28 ± 0.01
	zeta potential (mV)	–21 ± 1	–20 ± 2	–19 ± 1	–19 ± 2

Table 5 Particle size and zeta potential of 5 % CoQ10-loaded usNLC by PCS analysis at 3 different storage conditions for 3 months (z-average is a mean diameter and PI is a size distribution).

Storage conditions	Parameter	Day 1	Day 15	Day 30	Day 90
4 ± 2 °C	**z-average (nm)**	80 ± 1	79 ± 1	79 ± 1	81 ± 1
	PI	0.13 ± 0.02	0.14 ± 0.03	0.15 ± 0.03	0.15 ± 0.03
	zeta potential (mV)	–34.3 ± 1	–35 ± 3	–31 ± 2	–31 ± 0
20 ± 2 °C	**z-average (nm)**	81 ± 2	80 ± 2	80 ± 1	80 ± 1
	PI	0.13 ± 0.02	0.13 ± 0.03	0.13 ± 0.02	0.13 ± 0.03
	zeta potential (mV)	–34 ± 2	–32 ± 2	–32 ± 3	–34 ± 3
40 ± 2 °C	**z-average (nm)**	85 ± 1	104 ± 1	130 ± 2	204 ± 6
	PI	0.14 ± 0.03	0.11 ± 0.04	0.18 ± 0.03	0.32 ± 0.06
	zeta potential (mV)	–31 ± 1	–29 ± 2	–29 ± 1	–29 ± 0

A trend of decrease in the absolute zeta potential of both formulations was found at 40 ± 2 °C, although this was not statistically significantly ($p > 0.05$). The possibility of a decrease in the absolute zeta potential and an increase in the particle size might have contributed to the mixed nonionic surfactant film at the oil/water interface, and could be deformed due to a decrease in the solubility of the nonionic surfactant in the water at an elevated temperature. Consequently, the deformation of the hydrophilic film of Tween® 80 on the particles might have occurred, leading it to be a less negative zeta potential value. As a consequence, the particles began to grow in size by coalescence, due to the change of a steric effect and the decrease in the strength of the static repulsion between particles. To prevent the coalescence of particles, the addition of protective colloids or dispersing agents should be considered in further investigations.

For chemical stability, the amount of CoQ_{10} in all formulations was assessed by HPLC. On the first production day (month 0), the amount of CoQ_{10} was assumed to be the initial concentration in the usNLC, and the percentages of the remaining CoQ_{10} in each formulation at different temperatures over 3 months were analyzed and represented in a bar graph, as shown in **Figure 10**.

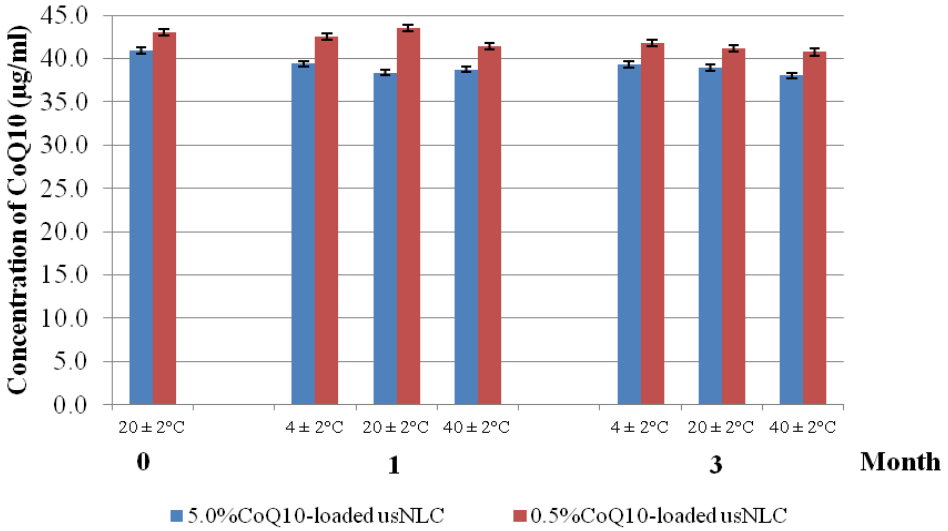

Figure 10 Short-term chemical stability of 0.5 % CoQ_{10}-loaded usNLC, 5 % CoQ_{10}-loaded usNLC at different storage temperatures for 3 months (n = 3).

From this set of HPLC data, the formulation of 0.5 % CoQ_{10}-loaded usNLC showed a higher concentration of the active compound at all different storage conditions of the temperature for 3 months, compared to another formulation. However, a good chemical stability of CoQ_{10} was found in both formulations at 4 ± 2 °C and room temperature, while the possibility of a decrease in the remaining amount of CoQ_{10} was found at 40 ± 2 °C in both formulations. This can be explained by the temperature effect, where a high temperature influenced the chemical stability of CoQ_{10} for a longer period of time in previous studies [20,30] finding a large extent degradation of CoQ_{10} at a temperature around 40 °C for at least 12 months. In addition, this effect can be described by the Arrhenius equation. The increasing temperature leads to an extension of the reaction rate of the chemical degradation of active substances [31]. Consequently, the active compounds should be stored at low temperatures, for good chemical stability.

From PCS and HPLC results, it can be assumed that the temperature influenced the physicochemical stability of CoQ_{10}-loaded usNLC. Additionally, the kinetic energy and electrostatic force

also affected the physicochemical properties of both formulations at an elevated temperature. For an extended time period of the final product, both formulations of CoQ_{10}-loaded usNLC are therefore recommended to be stored in the dark at low-temperature conditions.

Conclusions

CoQ_{10}-enriched shells of usNLC with smaller particle sizes tended to have higher antioxidant capacity than usNLC with larger paticle sizes in DPPH and biological KRL tests. Both formulations exhibited a good physicochemical stability at 4 and 20 °C for 3 months. However, the pro-oxidative effect of CoQ_{10} was shown at a high concentration in the KRL results, so this effect should be thoroughly investigated *in vivo* to ensure an effective and a safe use of CoQ_{10} in further studies.

Acknowledgements

We gratefully acknowledge Pharmasol GmbH, Berlin, Germany, for supporting the instrument and experiment operations, and the University of Phayao, Phayao, Thailand, for providing the financial support for this research.

References

[1] CA Boicelli, C Ramponi, E Casali and L Masotti. Ubiquinones: Stereochemistry and biological implications. *Membrane Biochem*. 1981; **4**, 105-18.
[2] P Mitchell. Possible molecular mechanisms of the protonmotive function of cytochrome systems. *J. Theor. Biol.* 1976; **62**, 327-67.
[3] G Lenaz, R Fato, G Formiggini and ML Genova. The role of Coenzyme Q in mitochondrial electron transport. *Mitochondrion Suppl.* 2007; **7**, S8-S33.
[4] A Mellors and AL Tappel. Quinones and quinols as inhibitors of lipid peroxidation. *Lipids* 1966; **1**, 282-4.
[5] A Boveris, E Cadenas and AOM Stoppani. Role of ubiquinone in the mitochondrial generation of hydrogen peroxide. *Biochem. J.* 1976; **156**, 435-44.
[6] K Muta-Takada, T Terada, H Yamanishi, Y Ashida, S Inomata, T Nishiyama and S Amano. Coenzyme Q_{10} protects against oxidative stress-induced cell death and enhances the synthesis of basement membrane components in dermal and epidermal cells. *Biofactors* 2009; **35**, 435-41.
[7] JH Rabe, AJ Mamelak, P McElgunn, WL Morison and DN Sauder. Photoaging: Mechanisms and repair. *J. Am. Acad. Derm*. 2006; **55**, 1-19.
[8] AR Fetoni, R Piacentini, A Fiorita, G Paludetti and D Troiani. Water soluble Coenzyme Q_{10} formulation (Q-ter) promotes outer hair cell survival in a guinea pig model of noise induced hearing loss (NIHL). *Brain Res*. 2009; **1257**, 108-16.
[9] J Zhang and S Wang. Topical use of coenzyme Q_{10}-loaded liposomes coated with trimethyl chitosan: tolerance, precorneal retention and anti-cataract effect. *Int. J. Pharm*. 2009; **372**, 66-75.
[10] N Baisaeng. 2013, Ultra-Small Lipid Nanocarriers Loaded with Coenzyme Q_{10}. Ph.D. Thesis. Freie Universität Berlin, Berlin, Germany.
[11] JC Schwarz and N Baisaeng. Ultra-small NLC for improved dermal delivery of coenyzme Q_{10}. *Int. J. Pharm*. 2013; **447**, 213-7.
[12] R Rossi, G Pastorelli and C Corino. Application of KRL test to assess total antioxidant activity in pigs: Sensitivity to dietary antioxidant. *Res. Vet. Sci*. 2003; **94**, 372-7.
[13] M Prost. 1992, Process for the Determination by Means of Free Radicals of the Antioxidant Properties of a Living Organism or Potentially Aggressive Agents. US patent 5135850.
[14] G Pastorelli, R Rossi, S Cannata and C Corino. Total antiradical activity in male castrated piglets blood: Reference values. *Ital. J. Anim. Sci*. 2009; **8**, 640-2.
[15] F Zülli, E Belser, D Schmid, C Liechti and F Suter. *Preparation and Properties of Coenzyme Q_{10} Nanoemulsions*. CH: Cosmetic Science Technology, Mibelle AG Biochemistry, 2006.
[16] RH Müller, SH Gohla and CM Keck. State of the art of nanocrystals: Special features, production,

nanotoxicology aspects & intracellular delivery. *Eur. J. Pharm. Biopharm*. 2011; **78**, 1-9.
[17] R Defay, I Prigogine, A Bellemans and DH Everett. *Surface Tension and Adsorption*. Longmans, London, 1966, p. 243-302.
[18] KL Jackson and GB McKenna. The melting behavior of organic materials confined in porous solids. *J. Chem. Phys*. 1990; **93**, 9002-11.
[19] H Bunjes, MHJ Koch and K Westesen. Effect of particle size on colloidal solid triglycerides. *Langmuir* 2000; **16**, 5234-41.
[20] V Teeranachaideekul, EB Souto, VB Junyaprasert and RM Müller. Cetyl palmitate based NLC for topical delivery of Coenzyme Q_{10}-development, physicochemical characterization and *in vitro* release studies. *Eur. J. Pharm. Biopharm*. 2007; **67**, 141-8.
[21] VB Junyaprasert, V Teeranachaideekul, EB Souto, P Boonme and RH Müller. Q_{10}-loaded NLC versus nanoemulsions: Stability, rheology and *in vitro* skin permeation. *Int. J. Pharm*. 2009; **377**, 207-14.
[22] K Westesen. Novel lipid-based colloidal dispersions as potential drug administration systems-expectations and reality. *Colloid Polym. Sci*. 2000; **278**, 608-18.
[23] P Swati, S Yogesh and J Sujata. Multivariate analysis of physicochemical characteristics of lipid based nanoemulsifying cilostazol quality by design. *Colloids Surf. B Biointerfaces* 2014; **115**, 29-36.
[24] H Nohl and L Gille. *Lysosomal ROS formation*. *Redox Report Comm. Free Radic. Res*. 2005; **10**, 199-205.
[25] J Terao. Antioxidant activity of β-carotene-related carotenoids in solution. *Lipids* 1989; **24**, 659-61.
[26] AL Lehninger. *The Mitochondrion*. W.A. Benjamin, New York, 1978.
[27] MS Giao, CI Pereira, SC Fonseca, ME Pintado and FX Malcata. Effect of particle size upon the extent of extraction of antioxidant power from the plants *Agrimonia eupatoria*, *Salvia* sp. and *Satureja montana*. *Food Chem*. 2009; **117**, 412-6.
[28] J Shen, XS Wang, M Garcia-Perez, D Mourant, MJ Rhodes and CZ Li. Effect of particle size on the fast pyrolysis of oil mallee woody biomass. *Fuel* 2009; **88**, 1810-7.
[29] Y Matsuda and R Masahara. Photostability of solid-state ubidecarenone at ordinary and elevated temperatures under exaggerated UV irradiation. *J. Pharm. Sci.* 1983; **72**, 1198-203.
[30] TR Kommuru, B Gurley, MA Khan and IK Reddy. *Int. J. Pharm*. 2001; **212**, 233-46.
[31] TR Kommuru, M Ashraf, MA Khan and IK Reddy. Stability and bioquivalence studies of two marketed formulations of coenzyme Q_{10} in beagle dogs. *Chem. Pharm. Bull.* 1999; **47**, 1024-8.